# The Stochastic Control of the F-8C Aircraft Using a Multiple Model Adaptive Control (MMAC) Method—Part I: Equilibrium Flight

MICHAEL ATHANS, FELLOW, IEEE, DAVID CASTAÑON, KEH-PING DUNN, MEMBER, IEEE, CHRISTOPHER S. GREENE, WING H. LEE, NILS R. SANDELL, JR., MEMBER, IEEE, AND ALAN S. WILLSKY, MEMBER, IEEE

*Abstract*—**The purpose of this paper is to summarize some results obtained for the adaptive control of the F-8C aircraft using the so-called MMAC method. The discussion includes the selection of the performance criteria for both the lateral and the longitudinal dynamics, the design of the Kalman filters for different flight conditions, the "identification" aspects of the design using hypothesis testing ideas, and the performance of the closed-loop adaptive system.**

## I. Introduction

The purpose of this paper is to present the results of Phase I of a study which deals with the evaluation of an advanced adaptive control method, the so-called multiple-model-adaptive-control (MMAC) method, in the context of a realistic problem, namely, the design of a stochastic regulator for both the longitudinal and lateral dynamics of the NASA F-8C aircraft. The results of the regulator study were necessary to

a) evaluate the potential of the method

b) provide guidance for Phase II, namely, the design of a true command and stability augmentation system which incorporates the effects of pilot commands and handling qualities.

The results of Phase II will not be reported in this paper, since the study is not as yet complete. It is important to stress, however, that the techniques described in this paper were suitably modified for the eventual design using the same overall approach.

The paper by Elliott [15] presents an overview of the NASA-F8 program. *It is important to stress that the results presented in this paper represent a research evaluation and feasibility study, strongly influenced by certain design guidelines whose purpose was to make the adaptive control problem difficult.* As explained in [15] the open-loop characteristics of the F-8C aircraft are such that complex stability augmentation systems are not required. This is also explained in the research of the Honeywell group; see [16]–[18]. Thus, the applications-oriented reader should keep in mind that the apparent complexity of the MMAC algorithm, as well as of some of the other approaches described in this issue, and notably that of Stein *et al.* [16], are purely due to the design assumptions imposed and are directed towards the development of an understanding of the utility of several advanced techniques for more exotic future aircraft and in other applications in which sophisiticated adaptive control algorithms are necessary. We repeat that the F-8 does not need anything fancy. Hence, the "practicality" of an F-8 design was judged in the context of whether or not it could be implemented using about half the resources of the IBM AP-101 flight computer (see [15]).

### A. Sensors

The major design decision which governed the design methodology and the eventual complexity of the adaptive control algorithm revolved about the sensors that were to be used. In the MMAC algorithm we only used the sensors shown in Table III. All accelerometers and gyros have triple redundancy on the F-8C while attitude gyros have dual redundancy. The general guidelines agreed upon by NASA and MIT/ESL was to utilize only very reliable sensors. For this reason, sensors that utilized air data such as sideslip and angle-of-attack vanes were not permitted. If airspeed and altitude sensors were used, then one could measure relatively accurately *dynamic pressure.* Prior studies by Honeywell [17] had shown that if dynamic pressure was known, then very simple gain scheduling could be carried out. For this reason, direct accurate measurements of airspeed, altitude, and dynamic pressure were *not* considered in the MMAC design or the Honeywell design [16] (in fact the main focus of the Honeywell design was indeed to estimate dynamic pressure from the reliable sensors). Attitude sensors were deemed undesirable by NASA [15], but they had to be used in order to resolve the components of the accelerometer readings.

TABLE I

| Flight Condition Number | Altitude (ft) | Mach Number | Dynamic Pressure (lb/ft$^2$) | Trim Angle of Attack (deg.) | Trim Elevator (deg.) |
|---|---|---|---|---|---|
| 5 | Sea level | 0.3 | 133.2 | 7.991 | −3.960 |
| 6 | Sea level | 0.53 | 416.0 | 2.989 | −2.495 |
| 7 | Sea level | 0.7 | 726.0 | 1.921 | −2.455 |
| 8 | Sea level | 0.86 | 1098.0 | 1.536 | −2.537 |
| 9 | Sea level | 1.0 | 1480.0 | 1.069 | −1.673 |
| 10 | 20 000 | 0.4 | 109.0 | 9.270 | −5.549 |
| 11 | 20 000 | 0.6 | 245.0 | 4.429 | −3.663 |
| 12 | 20 000 | 0.8 | 434.0 | 2.626 | −2.615 |
| 13 | 20 000 | 0.9 | 550.0 | 2.250 | −2.650 |
| 14 | 20 000 | 1.2 | 978.0 | 1.490 | −2.131 |
| 15 | 40 000 | 0.7 | 135.0 | 7.035 | −4.791 |
| 16 | 40 000 | 0.8 | 176.0 | 5.371 | −3.891 |
| 17 | 40 000 | 0.9 | 223.0 | 4.257 | −3.521 |
| 18 | 40 000 | 1.2 | 397.0 | 2.822 | −4.463 |
| 19 | 40 000 | 1.4 | 537.0 | 2.736 | −4.416 |
| 20 | 40 000 | 1.6 | 703.0 | 2.063 | −3.465 |

### B. Models

From the viewpoint of modeling, it is known that the dynamic state equations of an aircraft involve nonlinear differential equations (see Etkin [1]). However, the information given by NASA Langley Research Center (LRC) to the MIT/ESL team consisted of the specification of the *uncoupled*, linear time-invariant open-loop longitudinal and lateral dynamics of the F-8C aircraft associated with *equilibrium flight*. Table I gives a list of the 16 flight conditions that were available for the design. Thus, the general structure of the equations were of the form $\dot{x}(t) = Ax(t) + Bu(t)$. The numerical values of the elements of the $A$ and $B$ matrices can be found in a report by Gera [2], based upon wind tunnel tests, and a report by Wooley and Evans [3], based upon linearization of the nonlinear dynamics employed by NASA/LRC for their nonlinear simulation of the F-8C aircraft [15]. We remark at this point that the numerical values for the $A$ and $B$ matrices given in [2] and [3] are not identical, reflecting the fact that different sources were used to obtain

Manuscript received September 27, 1976; revised July 27, 1977. This research was carried out at the M.I.T. Electronic Systems Laboratory with support extended by NASA Langley Research Center under Grant NSG-1018. This paper is a revision of an earlier conference paper [19].

The authors are with the Electronic Systems Laboratory, Department of Electrical Engineering and Computer Science, Massachusetts Institute of Technology, Cambridge, MA 02139.

them. The design reported in this paper is based upon the linear models given in [3].

### C. Control Philosophy

As previously explained, this paper deals with the adaptive design of a system whose purpose is to maintain equilibrium flight conditions for the aircraft. The judgement was made that the equilibrium problem had to be understood first and the experience gained should be employed for the modifications necessary to incorporate pilot command inputs for both the longitudinal and lateral dynamics.[1]

However, all available evidence indicated that the desired response of the closed-loop aircraft varies with flight condition. The guidelines set forth called for a complete linear–quadratic–Gaussian (LQG) design for each flight condition which fully incorporated Kalman filters to handle sensor errors and to reconstruct the state variables (e.g., angle of attack, sideslip angle which could not be measured).

One of the first problems that had to be resolved was a definition of a quadratic performance criterion which changed in a natural way with different operating conditions. Such issues are discussed in more detail in Sections II and III of this paper. At this point, it suffices to state that the control and Kalman filter gains obtained for each operating condition were different. In the absence of dynamic pressure estimates the means for implementing gain scheduling are not obvious. This motivated the use of the MMAC algorithm as the main candidate; the (meager) theoretical basis for the MMAC algorithm is presented in Section V.

Since a digital implementation was necessary the LQG designs had to be carried out in both continuous [9] and discrete time [10] so that comparisons between them as a function of the sampling time could be obtained.

In closing these introductory remarks it is important to stress that the MMAC design differs in several key aspects from the Honeywell design (Stein *et al.* [16], also in this issue) although structurally they are similar. We shall attempt to point out the similarities and differences whenever appropriate. However, it is important to realize that the guidelines for the Honeywell design did *not* include Kalman filters to process the noisy sensor measurements; rather, simple low-pass filtering was deemed adequate. The basis MMAC design included Kalman filtering and hence it is more complex, requires more computation time, tuning, etc. It *can* be easily modified to remove the Kalman filter requirement for state reconstruction; however, this has not been done as yet.

A final philosophical comment can be made. Until now, the MMAC concept has been a theoretical development; MIT/ESL's efforts have tried to convert it into a practical design technique. MIT/ESL's design represented the "brute force" application of the MMAC concept; this approach is essential in understanding the limitations and implications of the theory, and in isolating areas where additional technical know-how must be incorporated. This approach contrasts with Honeywell's conservative approach, aimed at developing a complete, implementable design; the Honeywell design adapted a sophisticated parameter estimation method to a problem which already incorporated a great degree of simplification due to engineering knowhow. MIT/ESL's design effort has been very educational in providing valuable insight into a potentially useful design technique.

## II. Longitudinal Dynamics

### A. Introduction

In this section we present an overview of the LQG philosophy adopted for designing the regulator for the longitudinal dynamics. Attention is given to the development of the quadratic performance index and the subsequent model simplification using a short period approximation. The main concept that we wish to stress is that the quadratic performance criteria employed changed in a natural way with each flight condition. The surprising result was that the short period poles of the resultant longitudinal closed-loop system were characterized for all flight conditions by two constant damping ratios, one associated with all subsonic flight conditions and one associated with all supersonic flight conditions.

### B. The Longitudinal State Description

Because of a rate constraint saturation on the elevator rate [15], the control variable selected was the time rate of change of the commanded elevator rate ($\dot{\delta}_{ec}(t)$). This was integrated to generate the actual commanded elevator position ($\delta_{ec}(t)$) which was introduced to a first order servo with time constant of 1/12 s to generate the actual deviation of the elevator $\delta_e(t)$ from its trimmed value. The secondary actuator dynamics [15] were ignored. The elevator was then related to the four "natural" longitudinal state variables, namely, pitch rate $q(t)$ (rad/s), velocity error $u(t)$ (ft/s), perturbed angle of attack from its trimmed value $\alpha(t)$ (rad), and pitch attitude deviation from its trimmed value $\theta(t)$ (rad) [2]. In addition, a wind disturbance state $w(t)$ was included (see Appendix A). Thus the state vector $x(t)$ for the longitudinal dynamics was characterized by *seven* components

$$x'(t) \triangleq [q(t), u(t), \alpha(t), \theta(t), \delta_e(t), \delta_{ec}(t), w(t)] \tag{2.1}$$

and the control variable $u(t)$ was the commanded elevator rate

$$u(t) \triangleq \dot{\delta}_{ec}(t). \tag{2.2}$$

This led to a linear-time invariant characterization for each flight condition of the form

$$\dot{x}(t) = A_i x(t) + Bu(t) + L_i \xi(t) \tag{2.3}$$

where $\xi(t)$ was zero mean white noise, generating the wind disturbance and accounting for actuator model errors. The elements of $A_i$ and $L_i$ changed with each flight condition while

$$B = [0 \quad 0 \quad 0 \quad 0 \quad 0 \quad 1 \quad 0]'. \tag{2.4}$$

### C. The Longitudinal Cost Functional

In order to apply the standard steady-state LQG procedure [9] a quadratic performance index has to be selected. The general structure of the index was

$$J = \int_0^\infty x'(t) Q_i x(t) + u'(t) R_i u(t)\, dt. \tag{2.5}$$

Note that the weighting matrices $Q_i$, $R_i$ had to be different from flight condition to flight condition reflecting in a natural way that the pilot wants different handling qualities as the speed (and dynamic pressure) changes.

In the initial design it was decided that one should relate the maximum deviations of

pitch attitude $\theta_{\max}$
pitch rate $q_{\max}$
normal acceleration $a_{nz\max}$
maximum commanded elevator rate $\dot{\delta}_{ec\max}$

resulting in the following structure of the performance criterion:

$$J_{1,\mathrm{LON}} = \int_0^\infty \frac{a_{nz}^2(t)}{a_{nz\max}^2} + \frac{q^2(t)}{q_{\max}^2} + \frac{\theta^2(t)}{\theta_{\max}^2} + \frac{\dot{\delta}_{ec}^2(t)}{\dot{\delta}_{ec\max}^2}\, dt. \tag{2.6}$$

The normal acceleration $a_{nz}(t)$, in g's, was not used as a state variable. However, it is linearly related to some of the longitudinal state variables according to the formula

$$a_{nz}(t) = \frac{V_0}{g}[k_1 u(t) + k_2 \alpha(t) + k_3 \delta_e(t)] \quad \text{in g's}, \tag{2.7}$$

$V_0$ being the equilibrium speed. The constants $k_1$, $k_2$, $k_3$ can be calculated from the open-loop $A_i$ matrices and, hence, change with flight condition. Effectively, the structure of the criterion (2.6) implies that if at $t=0$ the maximum values of acceleration, pitch rate, or pitch attitude occurred, then one would be willing to saturate the elevator rate to remove them. For the preliminary design the following numerical values

[1] At this point we remark that pilot command designs have already been developed as Phase II of the project. The final evaluation of Phase II has not been completed as yet, and the results will be reported in future publications.

were selected (with the help of J. Elliott and J. Gera):

$$a_{nz\max}=6\text{g's},\quad q_{\max}=10\text{g}/V_0,\quad \theta_{\max}=6\text{g}/V_0a_{33},$$
$$\dot{\delta}_{ec\max}=0.435\text{ rad/s} \tag{2.8}$$

where $a_{33}$ is the (3,3) element of the open-loop longitudinal $A_i$ matrix.

Roughly speaking, this criterion means that one is willing to saturate the elevator rate (0.435 rad/s for the F-8C) if a normal acceleration of 6 g was felt, or a pitch rate equivalent to 10 g's, or a pitch error which if translated to angle of attack would also generate a 6 g normal acceleration.

The above numerical values were translated into the appropriate $Q_i$ matrix (nondiagonal, positive semidefinite) which changed from flight condition to flight condition, while $R_i=R=1/(0.435)^2$ for all flight conditions. Hence, the resulting LQ problem could be solved using available computer subroutines [11].

### D. Reduced Longitudinal Design

The design was modified for two reasons. First, the gain from the velocity state variable $u(t)$ was extremely small. Second, it was desirable to avoid using the pitch sensor. The pitch $\theta(t)$ is weakly observable from the system dynamics so that even if a Kalman filter was used in the absence of pitch measurements, large estimation errors would be obtained which would adversely affect the performance of the control system since there is significant feedback from the estimated pitch attitude. At any rate, since a pilot would fly the aircraft he would be able to control the pitch himself.

This led us to eliminating the velocity error $u(t)$ and the pitch $\theta(t)$ from the state equations and obtaining the "short period" approximation (five state variables). Since the pitch was not to be controlled the criteria (2.6) was modified to

$$J_{2,\text{LON}}=\int_0^\infty \frac{a_{nz}^2(t)}{a_{nz\max}^2}+\frac{q^2(t)}{q_{\max}^2}+\frac{\dot{\delta}_{ec}^2(t)}{\dot{\delta}_{ec\max}^2}\,dt \tag{2.9}$$

and the resultant LQ problem was resolved.

### E. Summary of Results

From the viewpoint of transient responses to the variables of interest (normal acceleration, pitch rate, and angle of attack) the transient responses to initial conditions were almost identical for both designs. Thus, the short period motion of the aircraft was dominated by the relative tradeoff between the maximum normal acceleration $a_{nz\max}$ and maximum pitch rate $q_{\max}$. This is consistent with the $C^*$ criterion [12].

When the short-period closed-loop poles were evaluated *for both designs* using the numerical values given by (2.8), we found the *unexpected result that the damping ratio was constant* (0.488) *for all 11 subsonic flight conditions, and also constant* (0.361) *for all the supersonic flight conditions*. The closed-loop natural frequency-increased with dynamic pressure.

Since no pole-placement techniques were employed (i.e., the mathematics were not told to place the closed-loop poles on a constant damping ratio line), we constructed a tradeoff by changing (decreasing) the maximum pitch rate $q_{\max}$. This would increase the pitch rate penalty in the cost functional, and one would expect a higher damping ratio. The following values of $q_{\max}$ were employed:

$$q_{\max}=10\text{g}/V_0, 8\text{g}/V_0, 6\text{g}/V_0, 4\text{g}/V_0. \tag{2.10}$$

Once more the constant damping ratio phenomenon was observed, i.e., for each value of $q_{\max}$ the short period closed-loop poles for all subsonic flight conditions fell on a constant damping ratio line, and similarly for all supersonic flight conditions. This was further verified by considering an additional 13 different flight conditions.

The numerical results are presented in Table II. The reason for this regularity of the solution of the LQ problem in terms of constant damping ratio properties remains unresolved.

TABLE II
DAMPING RATIO FOR CLOSED-LOOP SHORT PERIOD POLES AS A FUNCTION OF MAXIMUM PITCH RATE PENALTY $q_{\max}$ IN (2.6) OR (2.9)

| $q_{\max}$ | Damping Ratio for all Subsonic Conditions | Damping Ratio for all Supersonic Conditions |
|---|---|---|
| $10\text{g}/V_0$ | 0.488 | 0.361 |
| $8\text{g}/V_0$ | 0.530 | 0.402 |
| $6\text{g}/V_0$ | 0.552 | 0.449 |
| $4\text{g}/V_0$ | 0.587 | 0.498 |

## III. LATERAL DYNAMICS

### A. Introduction

In this section we present the parallel philosophy for the development of the regulator control system for the lateral dynamics. In this case the development of a performance criterion was not as straightforward as in the case of the longitudinal dynamics. For an extensive discussion see the S.M. thesis by Greene [13].

### B. The Lateral Dynamics State Model

The control variables selected for lateral control were

$$u_1(t)=\dot{\delta}_{ac}(t)=\text{commanded aileron rate (rad/s)} \tag{3.1}$$

$$u_2(t)=\dot{\delta}_{rc}(t)=\text{commanded rudder rate (rad/s)} \tag{3.2}$$

so that the control vector is defined to be

$$u(t)=[u_1(t)\quad u_2(t)]'. \tag{3.3}$$

The commanded aileron and rudder rates were integrated to generate the commanded aileron ($\delta_{ac}(t)$) and rudder ($\delta_{rc}(t)$) positions, respectively. For the F-8C aircraft the commanded aileron rate $\delta_{ac}(t)$ drives a first-order lag servo, with a time constant of 1/30 s, to generate the actual aileron position $\delta_a(t)$ (rad). The commanded rudder rate $\delta_{rc}(t)$ (rad) drives a first-order lag servo, with a time constant of 1/25 s, to generate the actual rudder position $\delta_r(t)$ (rad). The actual aileron and rudder position $\delta_a(t)$ and $\delta_r(t)$ then excite the four "natural" lateral dynamics state variables, namely, roll rate $p(t)$ (rad/s), yaw-rate $r(t)$ (rad/s), sideslip angle $\beta(t)$ (rad), and bank angle $\phi(t)$ (rad). In addition, a wind disturbance state variable $w(t)$ (see Appendix A) drives the equations in the same way as the sideslip variable. Again, secondary actuator dynamics [15] were ignored.

Thus, the state equations for the lateral dynamics are characterized by a nine-dimensional state vector $x(t)$ with components

$$x'(t)\triangleq[p(t),r(t),\beta(t),\phi(t),\delta_a(t),\delta_r(t),\delta_{ac}(t),\delta_{rc}(t),w(t)] \tag{3.4}$$

and the overall lateral dynamics take the form

$$\dot{x}(t)=A_ix(t)+Bu(t)+L_i\xi(t) \tag{3.5}$$

where the zero-mean white noise vector $\xi(t)$ generates the wind disturbance and compensates for modeling errors. Once more the matrices $A_i$, $L_i$ change with flight conditions [2], [3] while

$$B'=\begin{bmatrix}0&0&0&0&0&0&1&0&0\\0&0&0&0&0&0&0&1&0\end{bmatrix}. \tag{3.6}$$

### C. The Lateral Cost Functional

The lateral performance index used (after several iterations) weighted the following variables:

| | |
|---|---|
| lateral acceleration $a_y(t)$ | (g's) |
| roll rate $p(t)$ | (rad/s) |
| sideslip angle $\beta(t)$ | (rad) |
| bank angle $\phi(t)$ | (rad) |

versus
commanded aileron rate $\dot{\delta}_{ac}(t)$ (rad/s)
commanded rudder rate $\dot{\delta}_{rc}(t)$ (rad/s).

The lateral acceleration $a_y(t)$ is not a state variable. However, for small perturbations from equilibrium flight, it can be expressed as a linear combination of the lateral state variables and the trim angle of attack $\alpha_0$ by the following relation:

$$a_y(t)=\frac{V_0}{g}[(k_1-\alpha_0)p(t)+(k_2+1)r(t)+k_3\beta(t)$$
$$+k_4\phi(t)+k_5\delta_r(t)]-\phi(t)$$

where the constants $k_1,\cdots,k_5$ can be found from the lateral open-loop $A_i$ matrix and change with the flight condition.

The following structure of the quadratic performance criterion was established:

$$J_{\mathrm{LAT}}=\int_0^\infty \frac{a_y^2(t)}{a_{y\max}^2}+\frac{p^2(t)}{p_{\max}^2}+\frac{\beta^2(t)}{\beta_{\max}^2}+\frac{\phi^2(t)}{\phi_{\max}^2}+\frac{\dot{\delta}_{ac}^2(t)}{\dot{\delta}_{ac\max}^2}+\frac{\dot{\delta}_{rc}^2(t)}{\dot{\delta}_{rc\max}^2}\,dt. \tag{3.8}$$

The following maximum values were used:

1) Maximum lateral acceleration $a_{y\max}=0.25$ g's.
2) Maximum roll rate $p_{\max}=4V_0/\sqrt{10}g\,(a_{31}-\alpha_0)$.
3) Maximum sideslip angle $\beta_{\max}=4V_0/\sqrt{10}g\,a_{33}$.
4) Maximum bank angle $\phi_{\max}=0.233$ rad $(=15°)$.
5) Maximum commanded aileron rate $=1.63$ rad/s.
6) Maximum commanded rudder rate $=1.22$ rad/s.

See [13] for an extensive discussion of how this performance criterion was derived; $a_{31}$ and $a_{33}$ are obtained from the open-loop $A_i$ matrices.

There is no natural way of arriving at a simplified model for the lateral dynamics, as was the case with the longitudinal dynamics. Hence the bank angle cannot be eliminated. Although a bank angle sensor was deemed undesirable, the weak observability of the bank angle caused large state estimation errors in bank and sideslip angles if a bank angle sensor was not included. For these reasons, it was decided to employ a bank angle sensor and to penalize bank angle deviation to maintain the airplane near equilibrium flight.

Once more, the LQ problem can be solved. Notice that the use of the performance criterion (3.8) results in a state-weighting matrix $Q_i$ (nondiagonal) which changes with flight condition.

### D. Summary of Results

The above performance criterion gave reasonable responses for a variety of initial conditions. Its main characteristic is to reduce any lateral accelerations (by forcing the aircraft to execute coordinated turns) and to null out bank angle errors in a slower manner.

Once more we observed a constant damping ratio for the dutch roll mode (0.515) for all supersonic conditions, and (0.625) for all subsonic flight conditions.

## IV. Sensors, Kalman Filters, and Discrete LQG Compensators

### A. Introduction

The digital implementation of the control system requires the discrete-time solution of the LQG problem [10]. As we shall see in the next section, the MMAC approach requires the construction of a bank of LQG controllers, each of which contains a discrete Kalman filter (whose residuals are used in probability calculations and whose state estimates are used to generate the adaptive control signals). Hence, in this section we present an overview of the issues involved in the design of the LQG controllers based upon the noisy sensor measurements.

TABLE III
Sensor Characteristics

| Variable | Symbol | Standard deviation of additive white noise | |
|---|---|---|---|
| Pitch rate | $q$ | 0.489 | deg/s |
| Normal acceleration | $a_{n,z}$ | 0.06 | g's |
| Roll rate | $p$ | 1.956 | deg/s |
| Yaw rate | $r$ | 0.489 | deg/s |
| Bank angle | $\phi$ | 1.0 | deg |
| Lateral acceleration | $a_y$ | 0.04 | g's |

### B. The Sampling Interval

A sampling rate of 8 measurements/s was established. *Such a slow sampling rate was selected so as to be able to carry out in real time the multitude of real-time operations required by the MMAC method.*

### C. Sensors and Noise Characteristics

As explained in the Introduction, the guidelines for design excluded the use of air data sensors. Thus, measurements of altitude, speed, angle of attack, and sideslip angle were not available. After some preliminary investigations it was decided that sensors that depend on trim variables (elevator angle and pitch attitude) should not be used so as to avoid estimating trim parameters. (At this point we wish to remark that this was not the case with the Honeywell design which used elevator angle and generated trim estimates.) Table III lists the sensors and their accuracy characteristics that were used in this study. We stress that the sensors measure the true variables every 1/8 s in the presence of discrete, zero-mean white noise with the standard deviations given in Table III, which represent conservative estimates of sensor performance (see [15, Table II]).

Finally, we remark that in this study we assumed that all sensors were located at the CG of the aircraft.

### D. The Design of Kalman Filters

For each flight condition the steady-state discrete-time Kalman filter with constant gains was calculated for both the longitudinal and lateral dynamic models. The level of the plant white noise associated with the wind disturbance generation was selected so that we assumed that the aircraft was flying in cumulus clouds. (See Appendix A.)

The decision to use steady-state constant gain Kalman filters was made in order to minimize the computer memory requirements.

Finally, we remark that in view of the slow sampling rate, the continuous time filtering problem was carefully translated into the equivalent discrete problem [14].

The constant covariance matrices of the Kalman filter residuals, denoted by $S_{i\mathrm{LON}}$, $S_{i\mathrm{LAT}}$ for the longitudinal models and lateral models, were computed for each flight condition, denoted by $i$. As we shall see, these are important in the generation of the MMAC variables.

### E. The Design of the Discrete LQG Compensators

Through the use of the separation theorem one can design the discrete LQG compensators. This implied that the LQ problem defined in continuous time in Sections II and III had to be correctly transformed into the equivalent discrete-time problem in view of the slow measurement rate. Effectively, we have used the transformations given in [11] and [14].

### F. Recapitulation

For each flight condition, indexed by $i$, a complete discrete-time, steady-state, LQG compensator was designed for both the longitudinal and lateral dynamics. At 1/8th s intervals, each compensator generated the optimal control, namely, the optimal commanded elevator rate $\dot{\delta}_{ec}(t)$ for the longitudinal dynamics, and the optimal commanded aileron rate $\dot{\delta}_{ac}(t)$ and rudder rate $\dot{\delta}_{rc}(t)$ for the lateral dynamics, based upon the

noisy measurements of the appropriate sensors (see Table III) every 1/8 s.

Since we did not control the longitudinal phugoid mode, multirate sampling was not employed. At any rate, a sampling rate of 1/8 s is low for aircraft applications (the Honeywell design [16] used 50 measurements/s).

Because of the appropriate transformations of the continuous-time LQG problem to the discrete one, we noted no significant degradation in performance at this low sampling rate. No undesirable intersample behavior was noted.

The need for adaptive control is obvious because, if we assume that the aircraft is in flight condition $i$, but we use the LQG compensator obtained for flight condition $j$ for feedback control, this mismatching may generate either an unstable system or, often, at least a system with degraded performance. We also remark that such a mismatch instability is not only due to the control gains, but also due to the Kalman filter gains. Severe Kalman filter mismatching can lead to erroneous state estimates which in the MMAC design concept can generate bad control signals. It is important to stress that the problem of erroneous state estimates of the actually sensed variables by severely mismatched Kalman filters does not arise if one simply low passes the noisy sensor measurements, as in the Honeywell design.

## V. The MMAC Method

### A. Introduction

In this section we present the basic idea behind the MMAC method, and discuss how it was used in the F-8C context. In particular, we demonstrate how the information generated by the lateral and longitudinal sensors could be blended together. Finally, we make some remarks associated with the MMAC method and its general applicability to the design of adaptive control systems.

### B. The Basic Idea

Suppose one has $N$ linear, discrete-time stochastic time-invariant dynamic systems, indexed by $i=1,2,\cdots,N$, generating discrete-time measurements corrupted by white noise. Suppose that at $t=0$ "nature" selects one of these systems and places it inside a "black box." The true system generates a discrete set of measurements $z(t)$. The objective is to apply a control signal $u(t)$ to the true model.

The version of the MMAC method employed is as follows: one constructs a discrete-time steady-state LQG controller for each model; thus, one has a bank of $N$ LQG compensators. As shown in Fig. 1, each LQG compensator is driven by the actual control applied to the system $u(t)$ and driven by the actual noisy measurement vector $z(t)$. There are two signals of interest that each LQG compensator generates at time $t$:

1) the control vector $u_i(t)$, which would be the optimal control if indeed the system in the black box (viz. aircraft) was identical to the $i$th model

2) the residual or innovations vector $r_i(t)$ generated by each Kalman filter (which is inside the $i$th LQG compensator).

It turns out that from the residuals of the Kalman filters one can recursively generate $N$ discrete-time sequences denoted by $P_i(t)$, $i=1,2,\cdots,N$, $t=0,1,2,\cdots$, which, under suitable assumptions, are the conditional probabilities at time $t$, given the past measurements $z(\tau)$, $\tau \leqslant t$ and controls $u(\sigma)$, $\sigma \leqslant t-1$, that the $i$th model is the true one.

Assuming then that these probabilities are generated on-line (the formula will be given later) and given that each LQG compensator generates the control vector $u_i(t)$, then as shown in Fig. 1, the MMAC method computes the adaptive control vector $u(t)$, which drives the true system (viz. aircraft) and each of the Kalman filters inside the LQG compensators, by weighting the controls $u_i(t)$ by the associated probabilities, i.e.,

$$u(t)=\sum_{i=1}^{N} P_i(t)u_i(t). \tag{5.1}$$

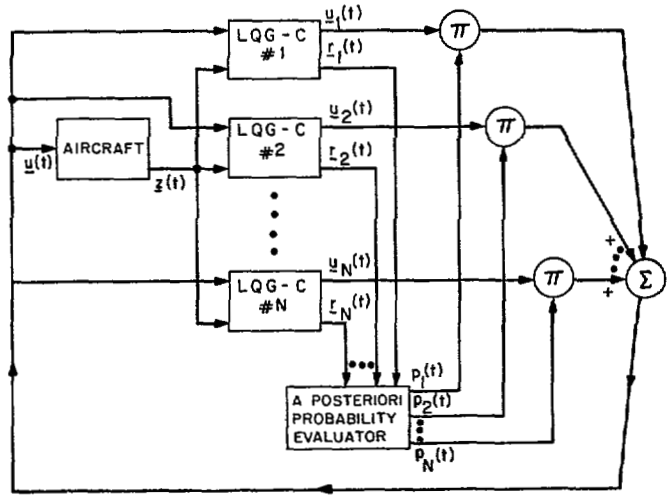


Fig. 1. Structure of MMAC system.

### C. Calculation of the Probabilities $P_i(t)$

Many adaptive control algorithms have strong identification components as well as control components. In the MMAC algorithm, the "identification" subsystem corresponds to the generation of the conditional posterior probabilities $P_i(t)$ that, based upon real-time sensor measurements, tell us which model appears to be the correct one.

We assume that at $t=0$, i.e., before any measurements are obtained, one has a set of prior probabilities

$$P_1(0),P_2(0),\cdots,P_N(0),P_i(0)\geqslant 0,\quad \sum_{i=1}^{N} P_i(0)=1 \tag{5.2}$$

that represent our "best guess" of which model is indeed the true one.

In our version of the MMAC method we have available the steady-state (constant) covariance matrix $S_i$ of the residuals associated with the $i$th Kalman filter. These $N$ residual covariance matrices are precomputable given the open-loop dynamics, the sensors, and the statistical characterization of the noises. Let $r$ denote the number of sensors; then we can precompute the $N$ scalars:

$$\beta_i^* \triangleq \left[(2\pi)^r \det S_i\right]^{-1/2}. \tag{5.3}$$

From the residual vector $r_i(t)$, i.e., the difference between the actual measurement and the predicted measurement at time $t$ generated by each Kalman filter, we generate *on-line* the $N$ scalars

$$m_i(t) \triangleq r_i'(t)S_i^{-1}r_i(t). \tag{5.4}$$

Then the probabilities at time $t$, $P_i(t)$, $i=1,2,\cdots,N$ are computed recursively from the probabilities at time $t-1$, $P_i(t-1)$, using the formula

$$P_i(t)=\frac{P_i(t-1)\,\beta_i^* \exp\{-m_i(t)/2\}}{\sum_{j=1}^{N} P_j(t-1)\,\beta_j^* \exp\{-m_j(t)/2\}} \tag{5.5}$$

with the initial probabilities $P_i(0)$ given. The probabilities $P_i(t)$ are then substituted into (5.1) to generate the adaptive control.

### D. Brief Historical Perspective

As explained in [4] there are several algorithms that employ a parallel structure of compensators to generate adaptive estimation and control algorithms. To the best of our knowledge the first effort along these lines was that of Magill whose Ph.D. dissertation culminated in [5]. Along similar veins Lainiotis and his students examined more general conditions for adaptive estimation (see [20] for a very recent survey and discussion); Lainiotis calls these *partitioned algorithms*. Such ideas are

also implicit in Aoki's book [25] and were also considered by Haddad and Cruz [24].

Multiple model type adaptive algorithms were considered by Stein [26] in his Ph.D. dissertation, by Saridis and Dao [27], and by Lainiotis [22], [23] whose original claims about true "nonlinear separation" properties were false. The properties of all these multiple model algorithms were examined by Willner [8] in his Ph.D. dissertation. The structure of the specific MMAC algorithm used in this paper is akin to that by Deshpande *et al.* [6] and Athans and Willner [7] in which they examined a hypothetical STOL example. All these multiple model adaptive estimation and control algorithms represent blends of stochastic estimation and dynamic hypothesis testing ideas. From an adaptive control point of view they are not dual control approaches (see [4] and [21]). The F-8 specific design by Stein *et al.* [16] can be also classified as a multiple model design.

### *E. Important Remarks*

1) It has been shown by Willner [8] that the MMAC method, i.e., generating the control via (5.1), is *not* optimal (it is optimal under suitable assumptions only for the last stage of the dynamic programming algorithm).

2) The MMAC algorithm is appealing in an ad hoc way because of its fixed structure and because its real-time and memory requirements are readily computable.

3) In the version used in this study, because we use steady-state Kalman filters rather than time-varying Kalman filters, the $P_i(t)$ are not exactly conditional probabilities.

4) We have been unable to find in the cited literature a rigorous proof of convergence of the claim that indeed the probability associated with the true model will asymptotically converge to unity.[2]

5) From a heuristic point of view, the recursive probability formula (5.5) makes sense with respect to identification. If the system is subject to some sort of persistent excitation, then one would expect that the residuals behave "regularly," i.e., the residuals of the Kalman filter associated with the correct model, say the $i$th one, will be "small," while the residuals of the mismatched Kalman filters ($j\neq i, j=1,2,\cdots,N$) will be "large." Thus, if $i$ indexes the correct model we would expect

$$m_i(t)\ll m_j(t) \qquad \text{all } j\neq i. \tag{5.6}$$

If such a condition persists over several measurements, the analysis of (5.5) shows that the "correct" probability $P_i(t)$ will increase, while the "mismatched model" probabilities will decrease. To see this, one can rewrite the formula (5.5) as follows:

$$P_i(t)-P_i(t-1)=\left[\sum_{j=1}^{N} P_j(t-1)\,\beta_j^*\exp\{-m_j(t)/2\}\right]^{-1} \cdot P_i(t-1)\left[(1-P_i(t-1))\,\beta_i^*\exp\{-m_i(t)/2\} - \sum_{j\neq i} P_j(t-1)\,\beta_j^*\exp\{-m_j(t)/2\}\right]. \tag{5.7}$$

Under our assumptions (5.6)

$$\exp\{-m_i(t)/2\}\approx 1 \tag{5.8}$$

$$\exp\{-m_j(t)/2\}\approx 0. \tag{5.9}$$

Hence, the correct model probability will grow according to

$$P_i(t)-P_i(t-1)\approx\frac{P_i(t-1)[1-P_i(t-1)]\,\beta_i^*}{\sum_{j=1}^{N} P_j(t-1)\,\beta_j^*\exp\{-m_j(t)/2\}}>0 \tag{5.10}$$

which demonstrates that as $P_i(t)\to 1$, the rate of growth slows down.

On the other hand, for the incorrect models, indexed by $j\neq i$, the same assumptions yield

$$P_j(t)-P_j(t-1)\approx\frac{-P_j(t-1)P_i(t-1)\,\beta_i^*}{\sum_{k=1}^{N} P_k(t-1)\,\beta_k^*\exp\{-m_k(t)/2\}}<0 \tag{5.11}$$

so that the probabilities decrease.

The same conclusions hold if we rewrite (5.7) in the form

$$P_i(t)-P_i(t-1)=\left[\sum_{j=1}^{N} P_j(t-1)\,\beta_j^*\exp\{-m_j(t)/2\}\right]-1 \cdot\left[P_i(t-1)\sum_{j\neq i} P_j(t-1)\left(\beta_i^*\exp\{-m_i(t)/2\} - \beta_j^*\exp\{-m_j(t)/2\}\right)\right]. \tag{5.12}$$

The above discussion points out that this "identification" scheme is crucially dependent upon the regularity of the residual behavior between the "matched" and "mismatched" Kalman filters.

6) The "identification" scheme, in terms of the dynamic evolution of the residuals, will not work very well if for whatever reason (such as errors in the selection of the noise statistics) the residuals of the Kalman filters do not have the above regularity assumptions. To be specific, suppose that for a prolonged sequence of measurements the Kalman filter residuals turn out to be such that

$$m_1(t)\approx m_2(t)\approx\cdots\approx m_N(t). \tag{5.13}$$

Then

$$\exp\{-m_i(t)/2\}\approx\alpha \qquad \text{for all } i. \tag{5.14}$$

Under these conditions and (5.12), we can see that

$$P_i(t)-P_i(t-1)\approx\frac{P_i(t-1)\sum_{j\neq i} P_j(t-1)(\beta_i^*-\beta_j^*)\alpha}{\sum_{j=1}^{N} P_j(t-1)\,\beta_j^*\alpha} = \frac{P_i(t-1)\sum_{j\neq i}(\beta_i^*-\beta_j^*)P_j(t-1)}{\sum_{j=1}^{N} P_j(t-1)\,\beta_j^*}. \tag{5.15}$$

Suppose that it turns out that one of the $\beta_i^*$'s, say $\beta_k^*$, is dominant, i.e.,

$$\beta_k^*>\beta_i^* \qquad \text{all } i\neq k. \tag{5.16}$$

In this case, the right-hand-side (RHS) of (5.15) will be negative for all $i\neq k$, which means that all the $P_i(t)$ will decrease, while the probability $P_k$ (associated with the dominant $\beta_k^*$) will increase. This behavior is very important, especially when the mathematical models used are substantially different from the real system. This point has not been discussed previously in the literature to the best of our knowledge, and deserves further attention independent of any results on convergence when the real system *is* one of the hypothesized models.

### *F. Application to the F-8C*

The MMAC method can be used in a straightforward manner using either longitudinal or lateral dynamics of the F-8C aircraft since we have designed both longitudinal and lateral LQG compensators for the available flight conditions, as we remarked in Section IV.

Under the assumptions of equilibrium flight the lateral and longitudinal dynamics of the aircraft become decoupled. Hence, from the individual banks of Kalman filters operating from the longitudinal and lateral sensors, respectively, one can obtain two sets of probabilities $P_i^{\text{LON}}(t)$ and $P_i^{\text{LAT}}(t)$ which theoretically could be combined into a single probability; the technical details can be found in [19]. Although this procedure is correct from the theoretical point of view, when evaluated via digital computer simulations, it was found to be deficient. The basic reason is

[2]Moore and Hawkes [28] developed some convergence results for convergence in the open-loop case.

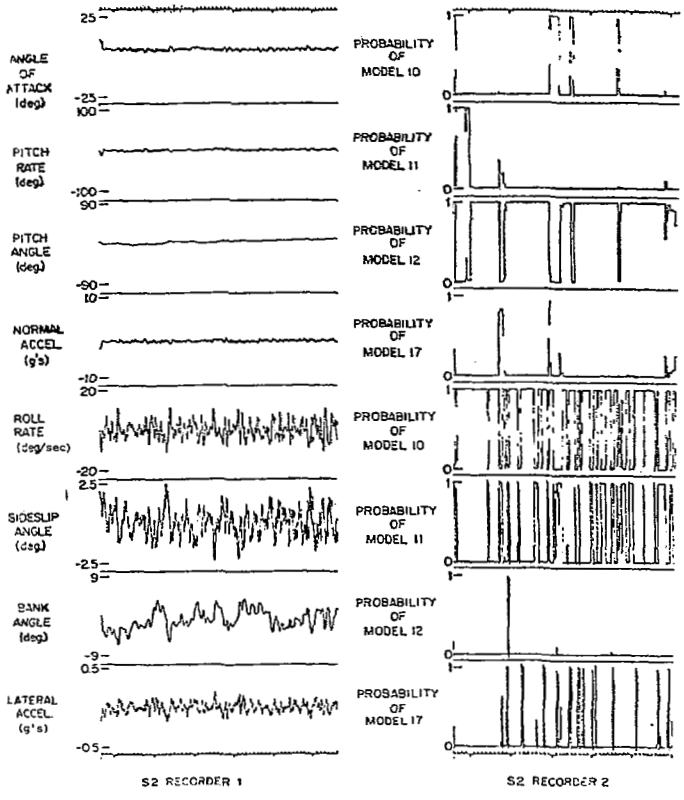


Fig. 2. Aircraft responses at FC 11; probabilities not filtered, 15 ft/s rms turbulence.

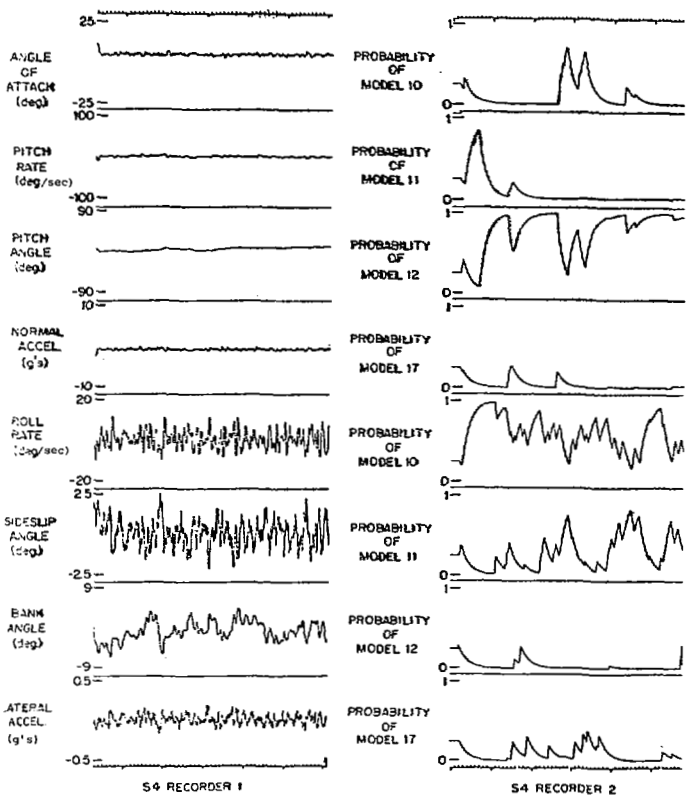


Fig. 3. Aircraft responses at FC 11; probabilities low-pass filtered 15 ft/s rms turbulence.

that under given operating conditions, the amount of information available for identification can be drastically different for the longitudinal and lateral systems. This is in agreement with the Honeywell [16] findings that demonstrate that it is very difficult to identify certain key lateral aerodynamic coefficients. Thus, in practice, the blending of the individual longitudinal and lateral probabilities into a single probability was abandoned. The causes for these errors in the overall probability calculation are due to $\beta^*$-dominance effects and inaccuracies in the tuning of the Kalman filters.

With these considerations, we designed two separate MMAC schemes for the longitudinal and lateral systems.

Other practical considerations were made in the design of the MMAC controllers. In theory, the probabilities of the individual models have zero as a lower bound. Under the hypothesis of the MMAC algorithm, where the true airplane condition is constant, it is desirable to have probabilities approach zero. In actual flight, the aircraft will change flight conditions; in order to keep the identification scheme sensitive to such changes, and to eliminate part of the influence of past information, the probabilities $P_i^{\mathrm{LON}}(t)$ and $P_i^{\mathrm{LAT}}(t)$ for the lateral and longitudinal systems are not allowed to be less than $10^{-4}$. This restriction makes the identification more rapid when changes occur.

After initial testing, we found that, under heavy turbulence (15 ft/s rms winds), the identification scheme was directly affected by the randomness of the turbulence, creating rapid changes in identification. Fig. 2 shows the identification changes and some of the relevant variables under heavy turbulence. With the aircraft at level flight, the main sources of excitation are the turbulence disturbances, so the identification reflects the random nature of these disturbances.

The oscillating identification was deemed undesirable as part of a control scheme. To eliminate it, the probabilities were low-pass filtered with a time constant of 2 by the formula

$$\bar{P}_i(t+1)=k\bar{P}_i(t)+(1-k)P_i(t+1) \tag{5.17}$$

where

$$k=e^{-1/16}=0.94041.$$

The probabilities $P_i(t)$ are computed according to (5.5). The probabilities $\bar{P}_i(t)$ are the low-pass filtered values used in the MMAC scheme. Thus, the actual control action applied to the aircraft is computed from the formula

$$u(t)=\sum_{i=1}^{N}\bar{P}_i(t)u_i(t). \tag{5.19}$$

Note that the identification sequence $P_i(t)$ is the same as it was previously. Thus, the identificaton scheme is not slowed down by the introduction of these low-pass filters. The probabilities $\bar{P}_i(t)$ are used strictly for the purposes of obtaining a smoother control action. The effect of the low-pass filter is to smooth out the fast transitions in identification to produce a smoother control action, thereby improving the handling qualities of the aircraft; see Fig. 3.

The final modification was implemented to alleviate the $\beta^*$-dominant behavior. We found that the cases where the $m_i(t)$ were all approximately equal were cases when all $m_i(t)$ were small (usually during calm, equilibrium flight). The magnitude of $m_i(t)$ represents the information available in the system for identification. Recognizing this pattern, we did not update the probabilities $P_i(t)$ when all of the residual products $m_i(t)$ were smaller than a given threshold; the threshold was set at different levels for the lateral and longitudinal systems. That is,

$$P_i(t+1)=P_i(t) \qquad \text{if } m_j(t)\leqslant T \text{ for all } j=1,\cdots,N. \tag{5.20}$$

The value of $T$ was determined in a trial and error fashion. Typical values used were 10 for the longitudinal system and 50 for the lateral system.

### G. Discussion

It should be immediately obvious that if the MMAC method is applied for the control of the F-8C aircraft (or any other physical system for that matter), one violates a multitude of theoretical assumptions. The effect of these upon the performance of an overall system is difficult to establish on an analytical basis because the MMAC system, in spite of

its simple structure, represents an extremely nonlinear system. Hence, one has to rely on extensive simulation results in order to be able to make a judgment of the performances of the overall algorithm.

Since the aircraft *never* coincides with the mathematical models (recall the discussion on the differences in the data given in [2] and [3]),the $P_i(t)$ are not truly posterior probabilities. Rather, they should be interpreted as time sequences that have a reasonable physical interpretation. Hence, in our opinion, the evaluation of the MMAC method solely by the detailed dynamic evolution of the $P_i(t)$ is wrong. Rather it should be judged by the overall performance of the control system. In the case of the regulator, this is easy since one can always compare the response of the MMAC system with that which was designed explicitly for that flight conditions and compare the results.

One of the biggest sources of coupling between the identification and the generation of the adaptive control that has to be considered in detail pertains to the use of Kalman filters to process the raw sensor data. The calculation of the adaptive control given by (5.1) can be rewritten as

$$u(t) = \sum_{i=1}^{N} P_i(t) G_i \hat{x}_i(t|t) \tag{5.21}$$

where the probabilities $P_i(t)$ are the same as in Section V-B, the matrices $G_i$ are the optimal control gains obtained from the solution of the linear-quadratic problem for the $i$th model, and $\hat{x}_i(t|t)$ are the state estimates generated by the $i$th Kalman filter. In the case of any identification errors, not only is one using the wrong control gains, but also the wrong state estimates. A "wrong" Kalman filter can generate erroneous state estimates and hence the control (5.21) can be severely in error, so that it may temporarily destabilize the aircraft. Under the design ground rules for the MIT/ESL team, Kalman filters had to be used to process the data, and very little could be done to avoid the effects of erroneous state estimates in the calculation of the adaptive control. The Honeywell design [16] was different. A bank of Kalman filters was used in the identification scheme, but not in state estimation. The Honeywell control system design used only low-pass filtered sensor signals and, hence, the generation of the Honeywell adaptive control was sensitive to the identification accuracy, but *not* to Kalman filter state estimation errors.

There are several unresolved problems as yet which pertain to the total number of models to be used at each instant of time, how these models are to be selected, how they should be scheduled in the absence of any air data, and how one can arrive at a final design that meets the speed-memory limitations of the IBM AP-101 computer which is used in the NASA F-8C DFBW program. Preliminary investigations indicate that an MMAC controller with four models in each system is feasible, with a sampling rate of 8 samples/s.

We hope that some of the simulation results and discussion presented in the sequel can contribute some understanding concerning the MMAC method as a design concept.

## VI. Simulation Results

### A. Introduction

A variety of simulations have been performed using a nonlinear model of the F-8C aircraft developed at NASA/LRC. These simulations have been conducted at several altitudes, airspeeds, and levels of turbulence. The simulation results shown here are typical. They have been selected to illustrate

1) the speed of identification of the MMAC algorithm
2) the overall performance of the MMAC system.

Some remarks about the MMAC method are given in the Conclusions.

### B. The Simulation Results

The simulations reported in this paper were conducted at an altitude of 20 000 ft, at subsonic speed (Mach 0.6) corresponding to flight condition 11 in Table I. The turbulence model described in Appendix A was used in some experiments at cumulus level turbulence. All models used in the MMAC controllers are given equal *a priori* probabilities of being the true model. Additionally, all measurements used in the MMAC system were noise-corrupted at the levels typical of actual F-8C sensors (Table III).

*Experiment 1:* This is a set of nonlinear simulations where the aircraft is subjected initially to a combined 6° angle of attack (alpha-gust) and 2° sideslip angle (beta-gust) perturbation. The Kalman filter states are initially set to zero, so that the initial perturbations are not readily estimated. In this experiment, the aircraft is not subjected to any turbulence.

Four simulations are illustrated in Figs. 4–6. The first simulation, indexed $A$, describes the *open-loop* response of the aircraft to the combined perturbations. The second simulation, indexed $B$, describes the closed-loop response of the aircraft with *perfect* identification of the flight condition. The third simulation, indexed $C$, describes the responses of the aircraft controlled with an MMAC controller which includes the true flight condition as one of its hypotheses. The fourth simulation, indexed $D$, describes responses of the aircraft controlled by an MMAC controller which does not include the true flight condition as a hypothesis.

Fig. 4 shows the pitch rate responses, Fig. 5 shows the normal acceleration responses, and Fig. 6 contains the lateral acceleration responses. Note the close correspondence of the MMAC responses to the perfect identification response. The initial perturbations are eliminated quickly, so that, with no noise driving the system, the aircraft is brought to equilibrium. The presence of sensor noise and small inaccuracies in the linear models of the nonlinear aircraft account for the small oscillation.

Fig. 7 contains the trajectories of the longitudinal identification probabilities for simulation $C$. Notice the quick identification of the true model within a very short period of time (less than 1 s), even though the Kalman filters are not correctly initialized and all measurements are noise-corrupted. The gradual increase in the probability of model 10 after 4.5 s is the $\beta^*$ dominant behavior of Section V; this occurs because, for this simulation only, the lower limit test of information was bypassed, so updating continued when all residuals were small.

Similar results were obtained with other initial conditions at other flight conditions. The most important point to note is the performance of the aircraft when controlled with an MMAC controller, compared with the perfect identification performance.

*Experiment 2:* Experiment 2 is essentially a repetition of experiment 1 when the aircraft is subjected to cumulus level turbulence. Figs. 8–10 contain the pitch rate, normal acceleration, and lateral acceleration responses of the aircraft. Again note that the responses of the MMAC controllers are very close to the responses of the perfect identification controller. Figs. 11 and 12 show the longitudinal and lateral *filtered* probabilities used for control when the MMAC controller contains flight condition 11 as a hypothesis. Note the gradual transitions in the identification compared with the sudden jumps of Fig. 7. The lateral system erroneously identifies flight condition 10 as the true flight condition; since flight condition 10 is "close" to flight condition 11, this error in identification is understandable. The performance is hardly affected by this misidentification, as evidenced by the closeness of traces $B$ and $C$ in Figs. 8–10.

Figs. 13 and 14 describe the filtered probabilities used in the MMAC controller when the true flight condition 11 is not included in the set of available models. The continuous transitions in the probabilities reflect the amount of excitation in the system caused by the cumulus disturbances. No clear identification is obtained in the transient period. However, the aircraft performance displayed in Figs. 8–10 is still satisfactory.

*Experiment 3:* This is a set of nonlinear simulations identical to the simulations obtained in experiment 2, except that the MMAC controllers use the identification probabilities in forming the control action without filtering. Fig. 2 contains a lengthy simulation of the MMAC controller performance with the true model included. Note the rapid oscillations in identification which occur after the initial transients die out, when the system is driven essentially by the turbulence. The faster oscillations in the lateral identification reflect the larger effect of turbulence on the lateral states. Fig. 3 describes the same simulation obtained from experiment 2, when filtered probabilities were used. The performance of the control systems is similar, and the control of Fig. 3 is smoother, as expected.

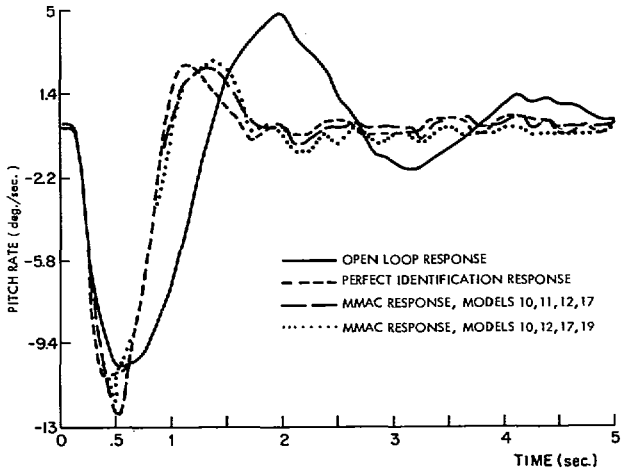


Fig. 4. Pitch rate responses at FC 11; no turbulence.

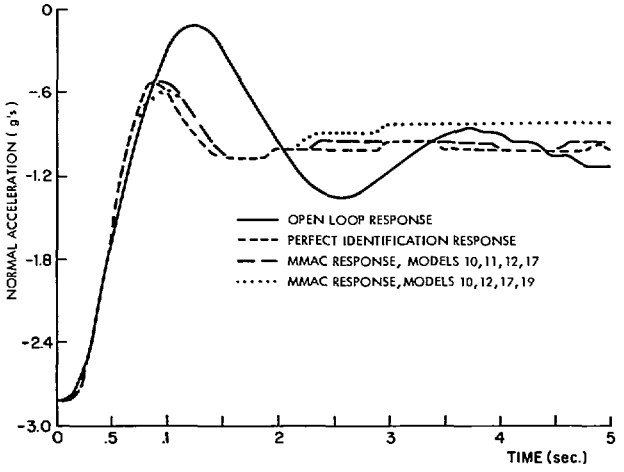


Fig. 5. Normal acceleration responses at FC 11; no turbulence.

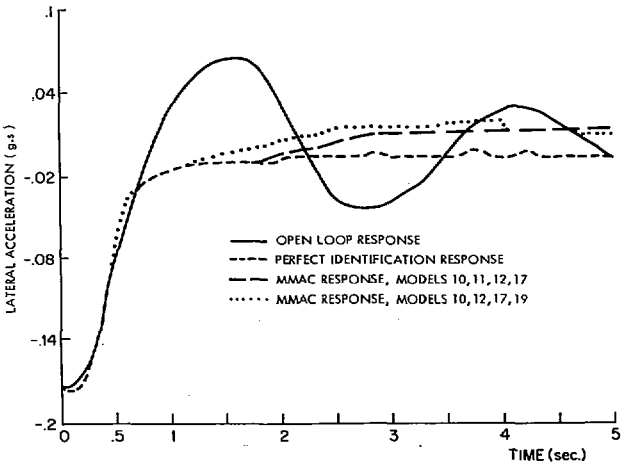


Fig. 6. Lateral acceleration responses at FC 11; no turbulence.

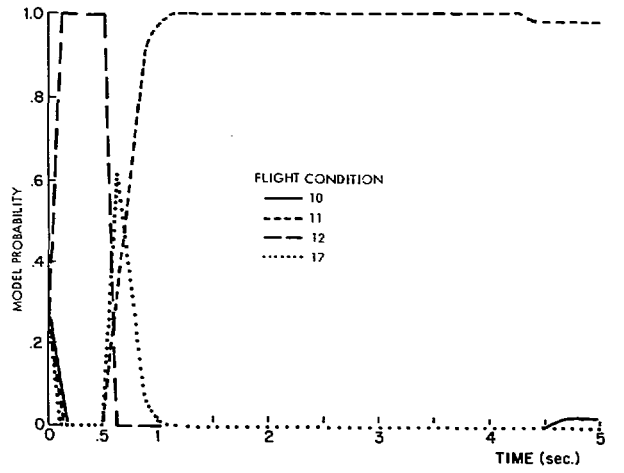


Fig. 7. Longitudinal system identification probabilities at FC 11; no turbulence.

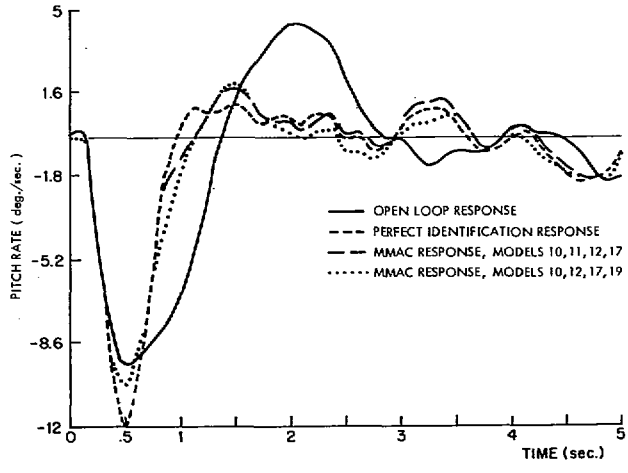


Fig. 8. Pitch rate responses at FC 11; 15 ft/s rms turbulence.

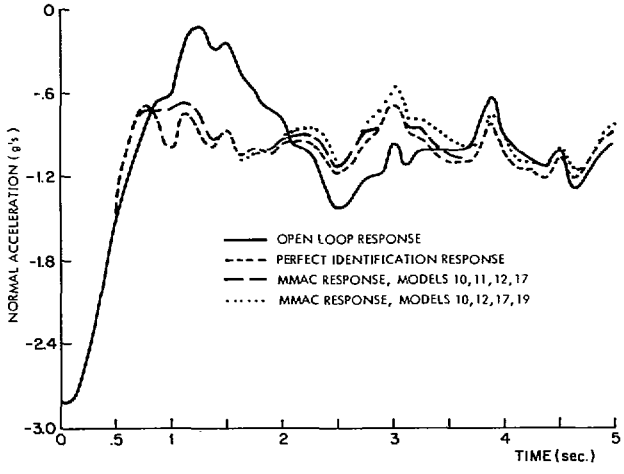


Fig. 9. Normal acceleration responses at FC 11; 15 ft/s rms turbulence.

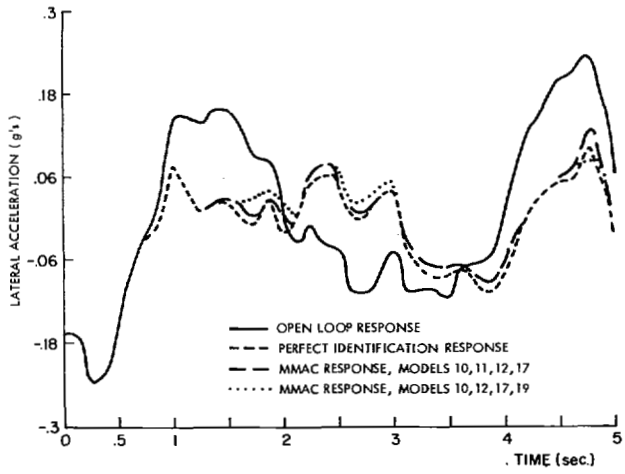


Fig. 10. Lateral acceleration responses at FC 11; 15 ft/s rms turbulence.

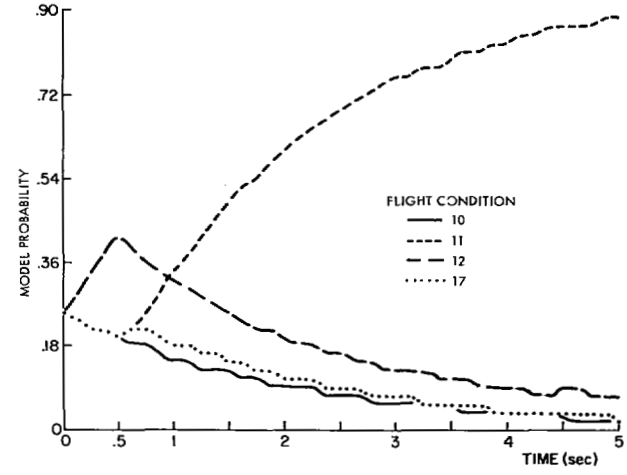


Fig. 11. Low-pass filtered longitudinal system probabilities at FC 11; 15 ft/s rms turbulence.

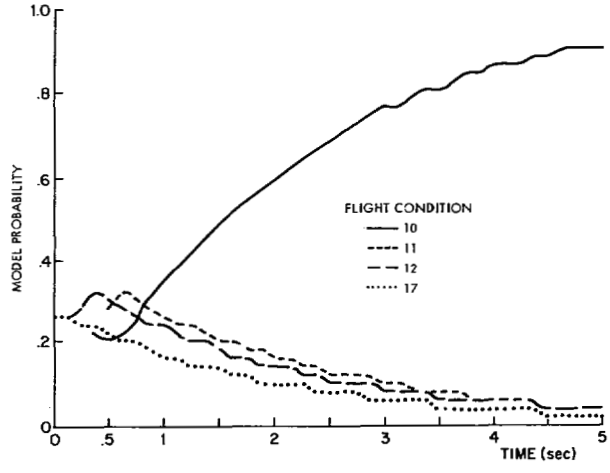


Fig. 12. Low-pass filtered lateral system probabilities at FC 11; 15 ft/s rms turbulence.

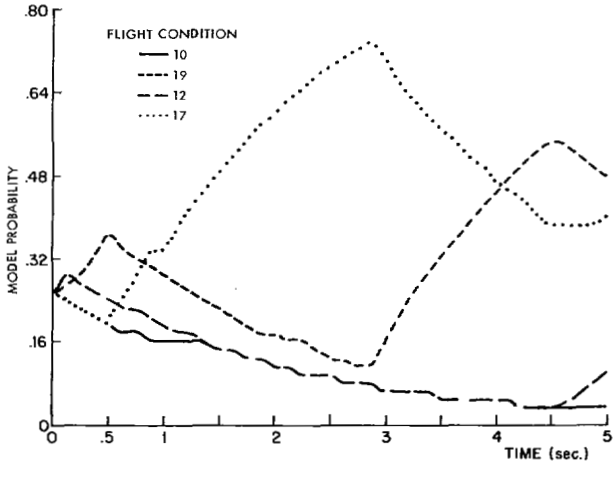


Fig. 13. Low-pass filtered longitudinal system probabilities at FC 11; 15 ft/s rms turbulence.

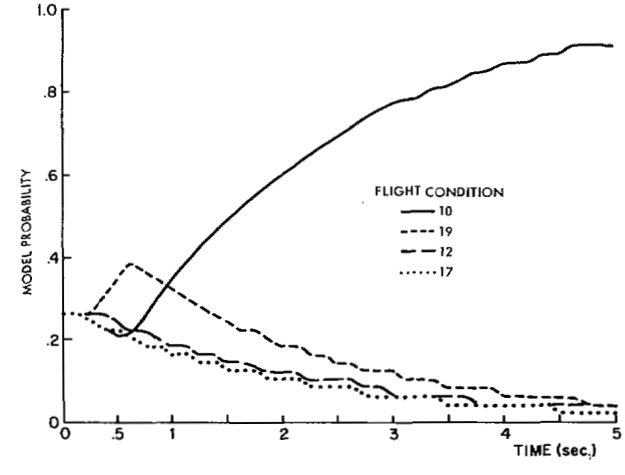


Fig. 14. Low-pass filtered lateral system probabilities at FC 11; 15 ft/s rms turbulence.

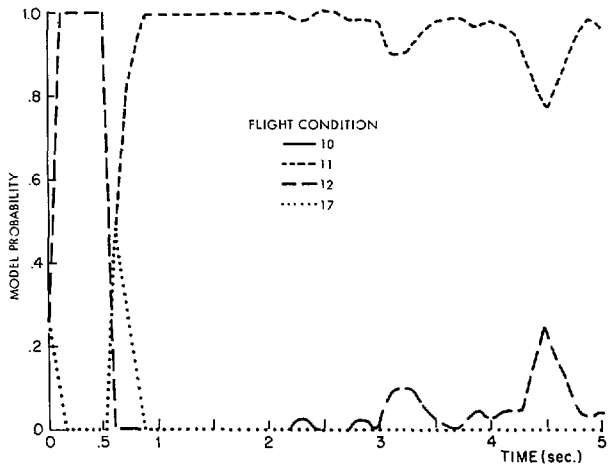


Fig. 15. Longitudinal system identification probabilities at FC 11; 15 ft/s rms turbulence.

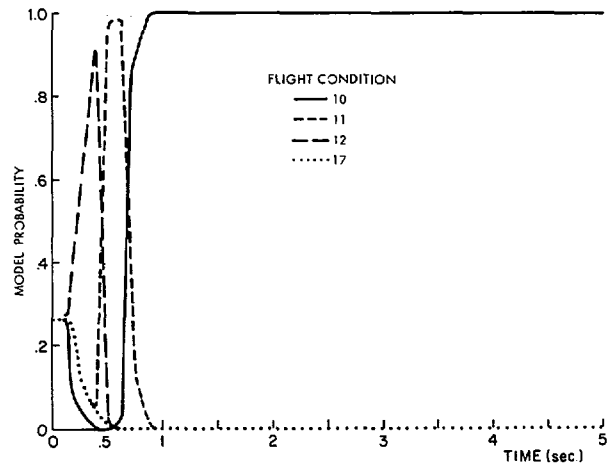


Fig. 16. Lateral system identification probabilities at FC 11; 15 ft/s rms turbulence.

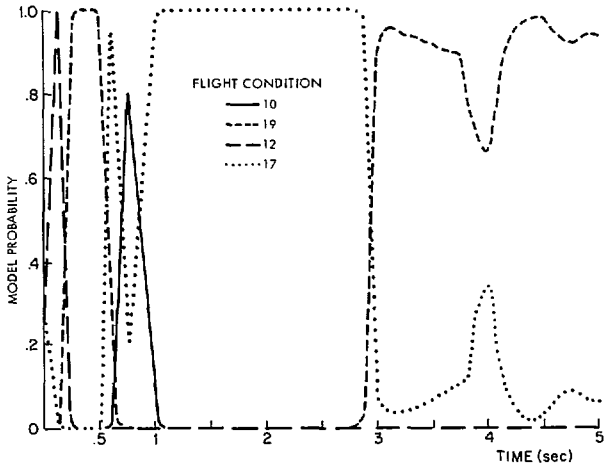


Fig. 17. Longitudinal system identification probabilities at FC 11; 15 ft/s rms turbulence.

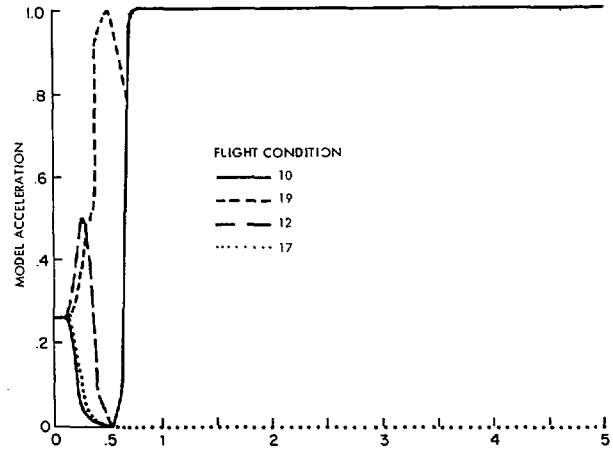


Fig. 18. Lateral system identification probabilities at FC 11; 15 ft/s rms turbulence.

Figs. 15 and 16 show the initial transients of the probabilities in Fig. 2. The filtered probabilities for this experiment are shown in Figs. 11 and 12. Similarly, Figs. 17 and 18 show the unfiltered identification probabilities when flight condition 11 is not a hypothesis. The filtered versions of these probabilities in experiment 2 are shown in Figs. 13 and 14.

Figs. 19–22 contain the angle-of-attack and sideslip angle responses of experiments 2 and 3. The closeness of these responses indicate that performance is not significantly affected by using low-pass filtered control actions. The open-loop and perfect identification responses are included to illustrate overall performance of the MMAC controllers.

## VII. Conclusions

The results of this feasibility study indicate that the MMAC approach is a reasonable candidate for aircraft adaptive control. The study, however, has pinpointed certain theoretical weaknesses in the MMAC algorithm as well as the need for using common sense pragmatic techniques to modify the design based upon "pure" theory.

The overall robustness and sensitivity of the MMAC algorithm appears to hinge upon careful tuning of the Kalman filters so that erroneous state estimates are not generated; in the MMAC approach they effect adversely both the identification accuracy and the actual values of the controls.

It appears that some sort of persistent excitation (test input signals) should be used in conjunction with the MMAC scheme, so that sufficient information for identification is always obtained. Unfortunately, no theoretical results are available as yet on a scientific basis for selecting the test input signals for the MMAC algorithm. Such questions cannot be answered until more fundamental research on the convergence of the MMAC algorithm is carried out.

The F-8 aircraft was chosen by NASA to be the test vehicle for evaluating the performance of adaptive control systems. However, the F-8 is not an aircraft which needs complex adaptive control systems. It is only when an accurate estimate of dynamic pressure is not available that the design of the control system becomes nontrivial, since ordinary gain scheduling cannot be used.

## Appendix A

*Wind Disturbance Model*

As remarked in Sections II and III, a continuous-time wind disturbance was included for both the lateral and longitudinal dynamics, corresponding to a state variable $w(t)$. In this Appendix we give the mathematical details of this model, which were kindly provided by J. Elliott of NASA/LRC, as a reasonable approximation to the von Karman model and the Haines approximation. It is important to realize that the wind disturbance model changes from flight condition to flight condition. The power spectral density of the wind disturbance is given by

$$\Phi_g = \frac{\sigma^2}{\pi}\frac{L}{V_0}\left[\frac{4}{4+\left(\frac{L}{V_0}\omega\right)^2}\right] \tag{A.1}$$

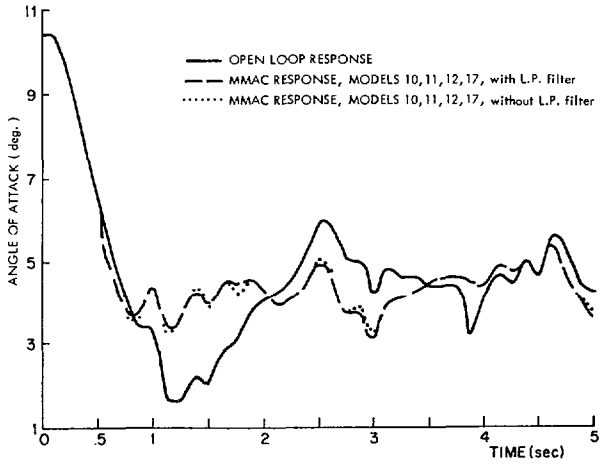


Fig. 19. Angle-of-attack responses at FC 11; 15 ft/s rms turbulence.

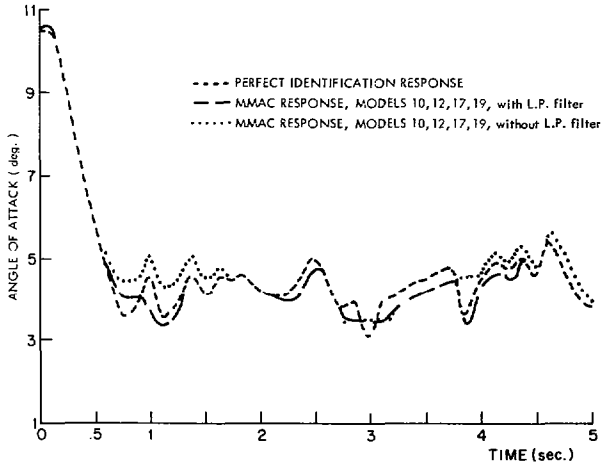


Fig. 20. Angle-of-attack responses at FC 11; 15 ft/s rms turbulence.

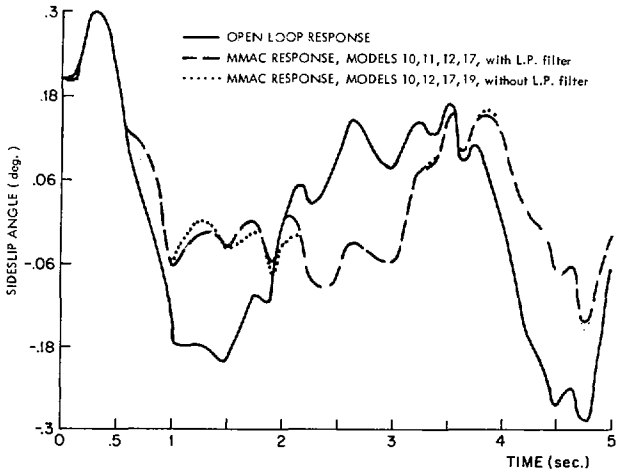


Fig. 21. Sideslip angle responses at FC 11; 15 ft/s rms turbulence.

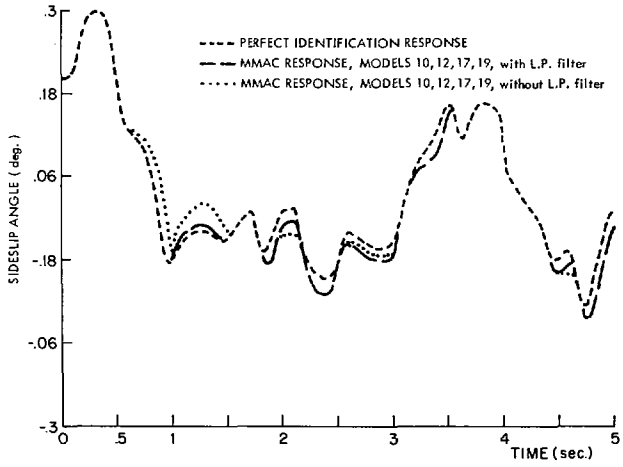


Fig. 22. Sideslip angle responses at FC 11; 15 ft/s rms turbulence.

where $L$, the scale length, is

$$L=\begin{cases}200\text{ ft at sea level}\\ 2500\text{ ft when altitude} > 2500\text{ ft}\\ \text{linearly interpolated in between.}\end{cases} \tag{A.2}$$

$V_0$ is the speed of aircraft in ft/s, $\omega$ in rad/s, and

$$\sigma=\begin{cases}6\text{ ft/s normal}\\ 15\text{ ft/s in cumulus clouds}\\ 30\text{ ft/s in thunderstorms.}\end{cases} \tag{A.3}$$

To obtain a state variable model, a normalized state variable $w(t)$ (in rad) is used as the wind state for both lateral and longitudinal dynamics. The state variable $w(t)$ is the output of a first-order system driven by continuous white noise $\xi(t)$ with zero mean. Thus the dynamics of the wind disturbance model are given by

$$\dot{w}(t)=-2\left(\frac{V_0}{L}\right)w(t)+\frac{2\sigma}{\sqrt{\pi L V_0}}\xi(t) \tag{A.4}$$

where $\xi(t)$ is zero-mean white noise with unity covariance function

$$E\{\xi(t)\xi(\tau)\}=\delta(t-\tau). \tag{A.5}$$

The design was obtained for the intermediate case $\sigma=15$ (cumulus clouds).

For the longitudinal dynamics the wind state $w(t)$ influences the dynamics in the same manner as the angle of attack. Thus, in the longitudinal state equations the wind state $w(t)$ enters the equations as follows:

$$\begin{cases}\dot{q}(t)=\cdots+a_{13}w(t)\\ \dot{v}(t)=\cdots+a_{23}w(t)\\ \dot{\alpha}(t)=\cdots+a_{33}w(t)\end{cases} \tag{A.6}$$

where $a_{13}$, $a_{23}$, $a_{33}$ can be found from the open-loop longitudinal $A$ matrix [3].

In the lateral dynamics the wind state $w(t)$ influences the dynamics in the same manner as the sideslip angle. Thus, in the lateral state equations the wind state $w(t)$ enters the equations as follows:

$$\begin{cases}\dot{p}(t)=\cdots+a_{13}w(t)\\ \dot{r}(t)=\cdots+a_{23}w(t)\\ \dot{\beta}(t)=\cdots+a_{33}w(t)\end{cases} \tag{A.7}$$

where $a_{13}$, $a_{23}$, $a_{33}$ can be found from the open-loop lateral $A$ matrix [3].

## Acknowledgment

This study was carried out under the overall supervision of Prof. M. Athans. The Program Managers were Dr. K.-P. Dunn and Dr. D. Castañon. C. S. Greene and Prof. A. S. Willsky were primarily responsi-

ble for the lateral system design. Prof. N. R. Sandell and W. H. Lee helped with the reduced-order longitudinal design. I. Segall and D. Orhlac did much of the programming.

We are indebted to J. R. Elliott of NASA/LRC who, as Grant Monitor, provided countless hours of technical discussions and direction and helped us formulate the performance criteria. In addition, we are indebted to the following staff of NASA/LRC for their help, criticism, and support: J. Gera, R. Montgomery, C. Wooley, A. Schy, and K. Hall.

## REFERENCES

[1] B. Etkin, *Dynamics of Atmospheric Flight.* New York: Wiley, 1972.
[2] J. Gera, "Linear equations of motion for F-8 DFBW airplane at selected flight conditions," NASA/Langley Res. Cent., Hampton, VA, F-8 DFBW Internal Document, Rep. 010-74.
[3] C. R. Wooley and A. B. Evans, "Algorithms and aerodynamic data for the simulation of the F8-C DFBW aircraft," NASA/Langley Res. Cent., Hampton, VA, unpublished rep. dated Feb. 5, 1975.
[4] M. Athans and P. P. Varaiya, "A survey of adaptive stochastic control methods," in *Proc. Eng. Foundation Conf. on Syst. Eng.*, New England College, Henniker, NH, Aug. 1975; also submitted to *IEEE Trans. Automat. Contr.*
[5] D. T. Magill, "Optimal adaptive estimation of sampled processes," *IEEE Trans. Automat. Contr.*, vol. AC-10, pp. 434–439, Oct. 1965.
[6] J. D. Desphande *et al.*, "Adaptive control of linear stochastic systems," *Automatica*, vol. 9, pp. 107–115, 1973.
[7] M. Athans and D. Willner, "A practical scheme for adaptive aircraft flight control systems," in *Proc. Symp. on Parameter Estimation Techniques and Appl. in Aircraft Flight Testing*, NASA Flight Res. Cen., Edwards, CA, TN-D-7647, Apr. 1973, pp. 315–336.
[8] D. Willner, "Observation and control of partially unknown systems," M.I.T. Electron. Syst. Lab., Cambridge, MA. Rep. ESL-R-496, June 1973.
[9] M. Athans, "The role and use of the stochastic LQG problem in control system design," *IEEE Trans. Automat. Contr.*, vol. AC-16, pp. 529–552, Dec. 1971.
[10] ——"The discrete time LQG problem," *Annals Economic and Social Measurement*, vol. 2., pp. 449–491, 1972.
[11] N. R. Sandell, Jr. and M. Athans, *Modern Control Theory: Computer Manual for the LQG Problem* (can be ordered through the M.I.T. Center for Advanced Engineering Study, Cambridge, MA).
[12] H. N. Tobie, E. M. Elliott, and L. G. Malcom, "A new longitudinal handling qualities criterion," presented at the 18th Ann. Nat. Aerospace Electron. Conf., May 16–18, 1966.
[13] C. S. Greene, "Application of the multiple model adaptive control method to the control of the lateral dynamics of an aircraft," M.S. thesis, Dep. Elec. Eng. and Comput. Sci., M.I.T., Cambridge, MA, May 1975.
[14] A. H. Levis, M. Athans, and R. Schlueter, "On the behavior of optimal sampled data regulators," *Int. J. Contr.*, vol. 13, pp. 343–361, 1971.
[15] J. R. Elliott, "NASA's advanced control law program for the F-8 digital fly-by-wire aircraft," this issue, pp. 753–757.
[16] G. Stein, G. L. Hartmann, and R. C. Hendrick, "Adaptive control laws for F-8 flight test," this issue, pp. 758–767.
[17] G. L. Hartmann *et al.*, "F8-C digital CCV flight control laws," NASA Contractor Rep. NASA CR-2629, Feb. 1976.
[18] G. L. Hartmann *et al.*, "F-8C adaptive flight control laws," Honeywell Fin. Rep., Contract NAS1-13383.
[19] M. Athans *et al.*, "The stochastic control of the F8-C aircraft using the multiple model adaptive control (MMAC) Method," in *Proc. 1975 IEEE Conf. on Decision and Contr.*, Houston, TX, Dec. 1975, pp. 217–228.
[20] D. G. Lainiotis, "Partitioning: A unifying framework for adaptive systems, Parts I and II," *Proc. IEEE*, vol. 64, Part I, pp. 1126–1142, Part II, pp. 1182–1197, Aug. 1976.
[21] E. Tse and Y. Bar-Shalom, "Actively adaptive control for nonlinear stochastic systems," *Proc. IEEE*, vol. 64, pp. 1172–1181, Aug. 1976.
[22] D. G. Lainiotis *et al.*, "Optimal adaptive control: A nonlinear separation theorem," *Int. J. Contr.*, vol. 15, pp. 877–888, 1972.
[23] D. G. Lainiotis *et al.*, "Optimal adaptive estimation: Structure and parameter adaptation," *IEEE Trans. Automat. Contr.*, vol. AC-16, pp. 160–170, Apr. 1971.
[24] A. H. Haddad and J. B. Cruz, Jr., "Nonlinear filtering for systems with unknown parameters," in *Proc. 2nd Symp. on Nonlinear Estimation Theory and Its Applications*, San Diego, CA, 1971, pp. 147–150.
[25] M. Aoki, *Optimization of Stochastic Systems.* New York: Academic, 1976, pp. 237–241.
[26] G. Stein, "An approach to the parameter adaptive control problem," Ph.D. dissertation, Purdue Univ., Lafayette, IN.
[27] G. N. Saridis and T. K. Dao, "A learning approach to the parameter self organizing control problem," *Automatica*, vol. 8, pp. 589–597, 1972.
[28] J. B. Moore and R. M. Hawkes, "Decision methods in dynamic system identification," presented at the IEEE Conf. on Decision and Contr., Houston, TX, Dec. 1975.

# An Implementable Digital Adaptive Flight Controller Designed Using Stabilized Single-Stage Algorithms

GURBUX ALAG AND HOWARD KAUFMAN, SENIOR MEMBER, IEEE

***Abstract*—Adaptive flight control systems are of interest because of their potential for providing uniform stability and handling qualities over a wide flight envelope despite uncertainties in the open-loop characteristics of the aircraft. Because of the potential for actual implementation of adaptive control algorithms using contemporary small digital computer equipment, a study has been made to define an implementable digital adaptive control system which can be used for a typical fighter aircraft. Towards such an implementation, an explicit adaptive controller, which makes direct use of on-line parameter identification, has been developed and applied to both the linearized and nonlinear equations of motion for the F-8 aircraft. This controller is composed of an on-line weighted least squares parameter identifier, a Kalman state filter, and a real model following control law designed using single-stage performance indices. The corresponding control gains are readily adjustable in accordance with parameter changes to ensure asymptotic stability if the conditions of perfect model following are satisfied, and stability in the sense of boundedness otherwise. Simulation experiments with realistic measurement noise indicate that the controller was effective in compensating for parameter variations and capable of rapid recovery from a set of erroneous initial parameter estimates which defined a set of destabilizing gains.**

Manuscript received October 18, 1975; revised March 28, 1977. This work was supported by NASA Grant NGR 33-018-183, administered by the Langley Research Center, Hampton, VA.

G. Alag was a Visiting Professor at the University of Houston, Houston, TX in 1976–1977.

H. Kaufman is with the Department of Electrical and Systems Engineering, Rensselaer Polytechnic Institute, Troy, NY 12181.

## I. INTRODUCTION

Fly-by-wire flight control systems have been of considerable interest to designers because of their advantages over mechanical linkages in coping with the complex control problems associated with high performance aircraft and space vehicles [1], [2]. Furthermore, with the present capabilities for incorporating integrated circuits into lightweight low cost minicomputers and microcomputers, digital implementation of fly-by-wire control becomes especially attractive. Digital logic is itself very reliable and with adequate redundancy incorporated into the design, such a system can be designed to insure adequate flight safety [3].

Another feature of digital implementation which makes it extremely advantageous is the potential for the implementation of complex control systems which incorporate high-order nonlinearities and which utilize time sharing for multiple-loop control. One such complex control structure is an adaptive system which is capable of on-line adjustment of the control parameters in response to changing flight characteristics. The desirability for such adaptive control systems has been established for